



Supplement of

Historical and future changes of surface ozone over China from CMIP6 models, including an assessment of present-day uncertainties in model prediction

Shuai Li et al.

Correspondence to: Hua Zhang (huazhang@cma.gov.cn)

The copyright of individual parts of the supplement might differ from the article licence.

Contents

Figure S1 – The Bias in surface O₃ concentrations simulated by CMIP6 models relative to TAP from 2015 to 2023 under different concentrations of PM_{2.5} components (including BC, NO₃, SO₄, NH₄, OM) in China.

Figures S2 – Changes in the annual mean surface O₃ concentrations for China and sub-regions from 2015–2100, across nine CMIP6 models and MME for the SSP3-7.0 scenario.

Figures S3 – Changes in the annual mean surface NO_x concentrations for China and sub-regions from 2015–2100, across nine CMIP6 models and MME for the SSP3-7.0 scenario.

Figures S4 – Changes in the annual mean surface CH₄ concentrations for China and sub-regions from 2015–2100, across nine CMIP6 models and MME for the SSP3-7.0 scenario.

Figures S5 – Changes in the annual total emissions of BVOCs for China and sub-regions from 2015–2100, across nine CMIP6 models and MME for the SSP3-7.0 scenario.

Figures S6 – Changes in the annual total emissions of NMVOCs for China and sub-regions from 2015–2100, across nine CMIP6 models and MME for the SSP3-7.0 scenario.

Figures S7 – Changes in the annual mean TAS concentrations for China and sub-regions from 2015–2100, across nine CMIP6 models and MME for the SSP3-7.0 scenario.

Figure S8 – The average pollutants concentrations and the proportion of exceeding the standard in China during 2015–2024.

Table S1 – CMIP6 variables and auxiliary datasets used in this study.

Table S2 – Summary of seasonal performance statistics of MME O₃ relative to TAP.

Table S3 – Annual correlation coefficients between individual CMIP6 models and TAP.

Table S4 – Meaning and characteristics of typical scenarios in CMIP6 in this study.

Table S5 – Multi-model mean changes in surface ozone concentrations over China and globally under historical and SSP scenarios.

Table S6 – Inter-ensemble variability of surface O₃ under SSP3-7.0 (2015–2023).



Figure S1 – The Bias in surface O₃ concentrations simulated by CMIP6 models relative to TAP from 2015 to 2023 under different concentrations of PM_{2.5} components (including BC, NO₃, SO₄, NH₄, OM) in China.

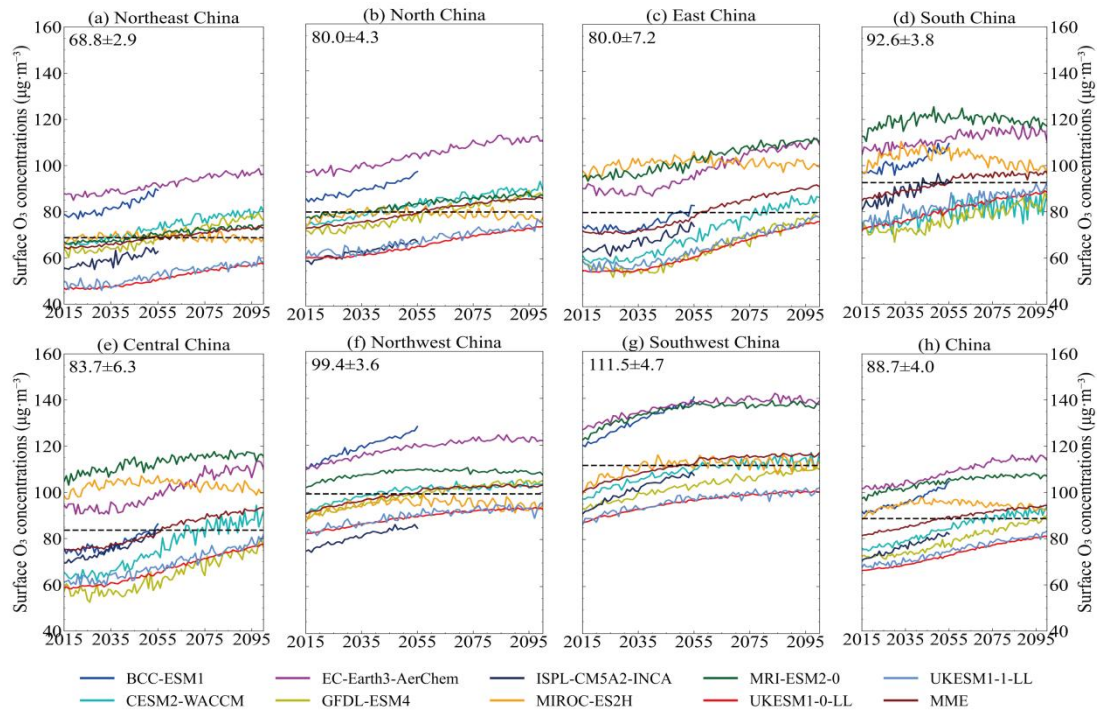


Figure S2 – Changes in the annual mean surface O₃ concentrations for China and sub-regions from 2015–2100, across nine CMIP6 models and MME for the SSP3-7.0 scenario. The black dashed line represents the MME of surface O₃ concentrations for 2015–2100, with the value (±1 SD) shown in the top left of each panel.

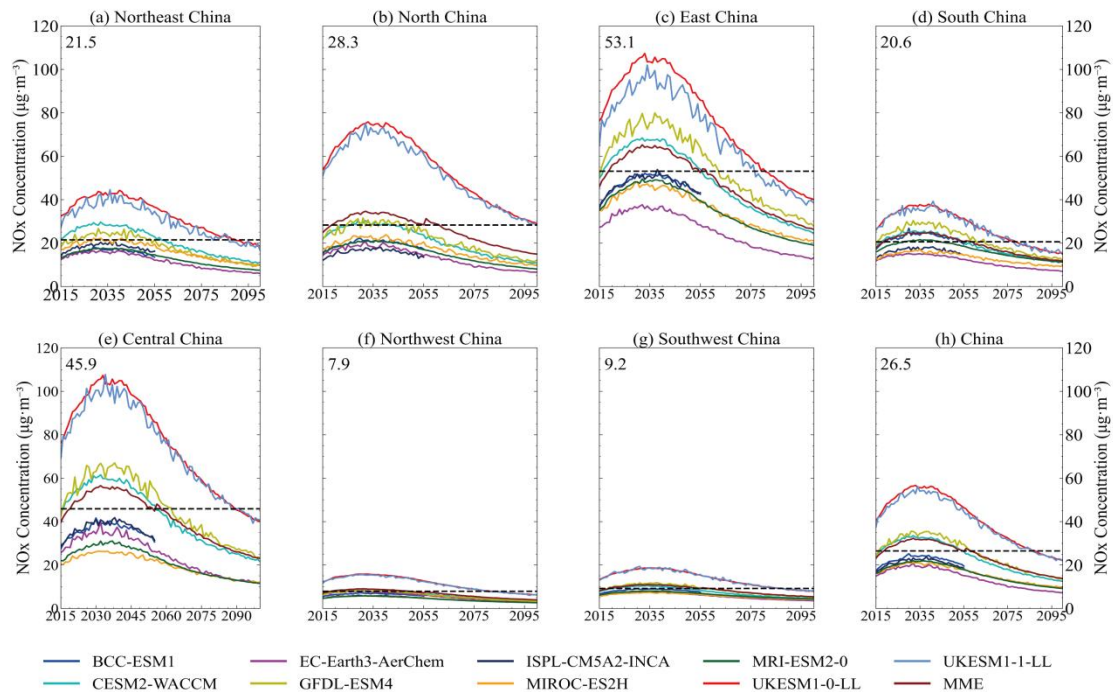


Figure S3 – Changes in the annual mean surface NO_x concentrations for China and sub-regions from 2015–2100, across nine CMIP6 models and MME for the SSP3-7.0 scenario. The black dashed line represents the MME of surface NO_x concentrations for 2015–2023, with the value shown in the top left of each panel.

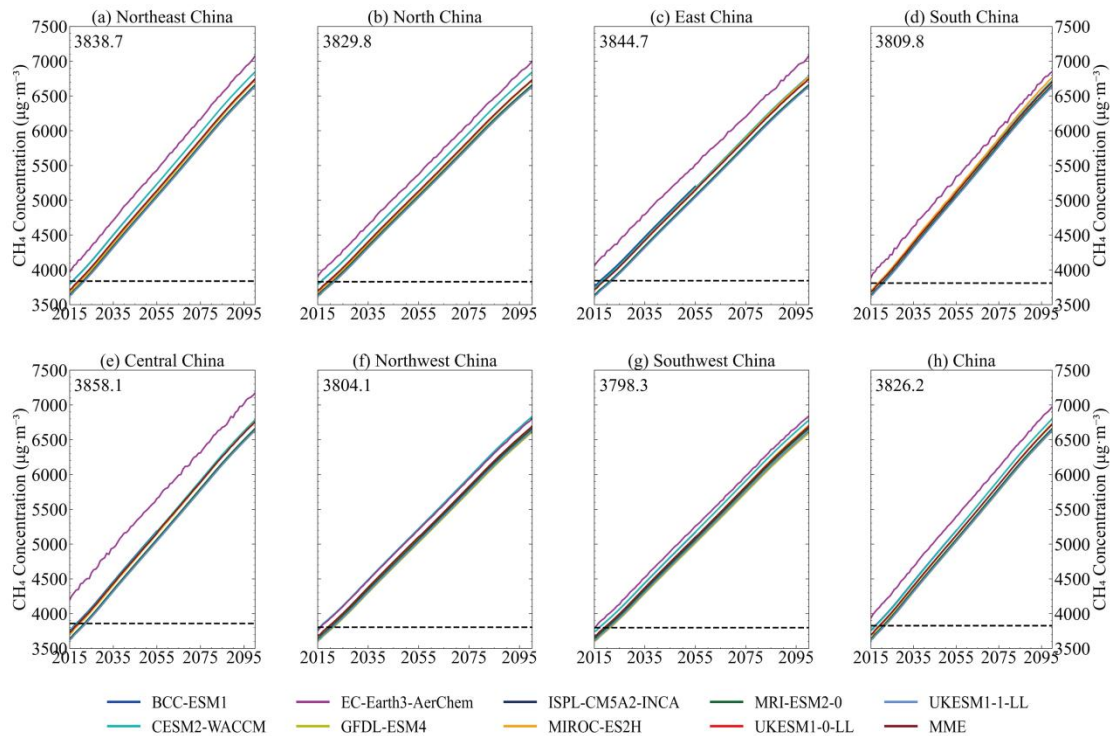


Figure S4 – Changes in the annual mean surface CH₄ concentrations for China and sub-regions from 2015–2100, across nine CMIP6 models and MME for the SSP3-7.0 scenario. The black dashed line represents the MME of surface CH₄ concentrations for 2015–2023, with the value shown in the top left of each panel.

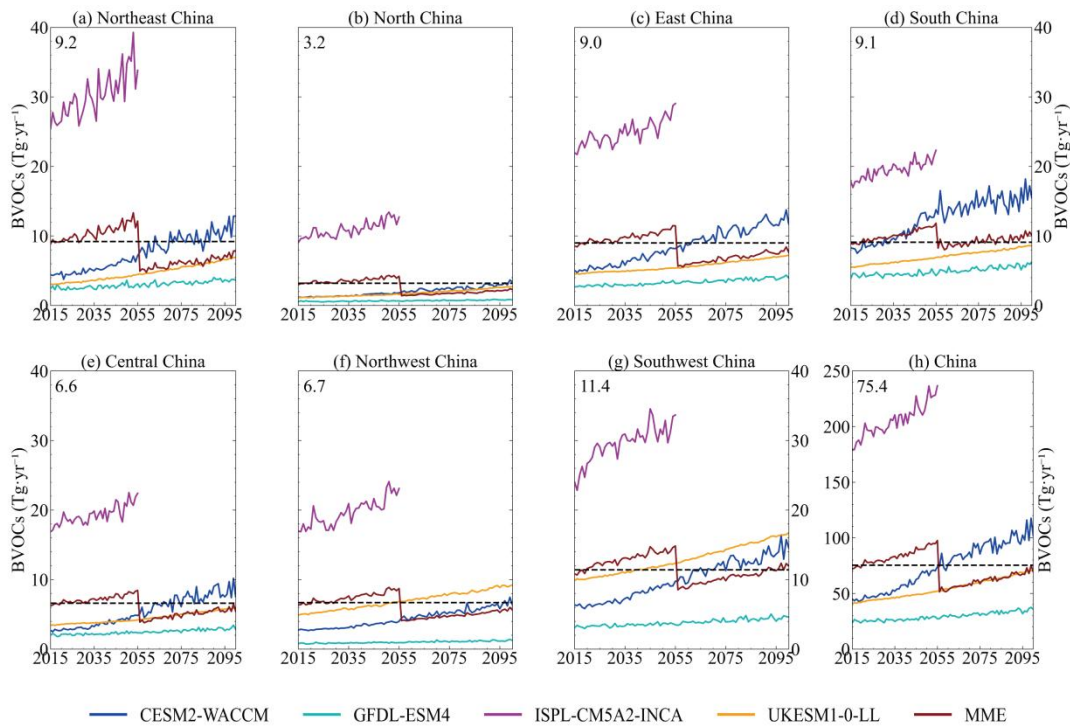


Figure S5 – Changes in the annual total emissions of BVOCs for China and sub-regions from 2015–2100, across nine CMIP6 models and MME for the SSP3-7.0 scenario. The black dashed line represents the MME of total BVOCs emissions for 2015–2023, with the value shown in the top left of each panel.

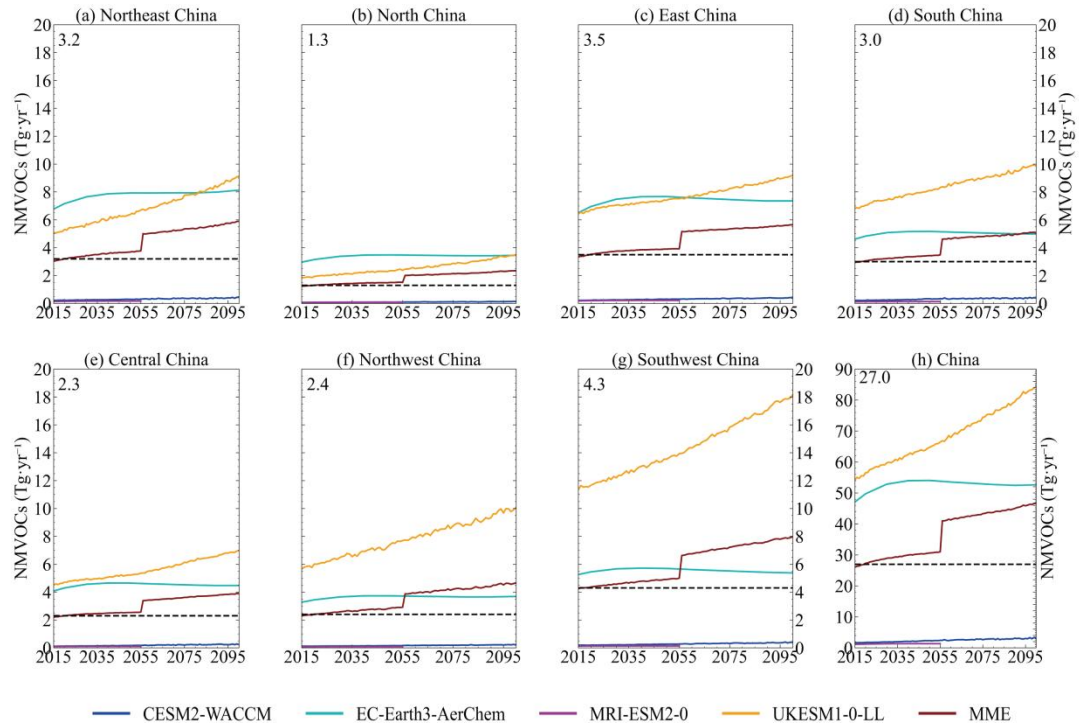


Figure S6 – Changes in the annual total emissions of NMVOCs for China and sub-regions from 2015–2100, across nine CMIP6 models and MME for the SSP3-7.0 scenario. The black dashed line represents the MME of total NMVOCs emissions for 2015–2023, with the value shown in the top left of each panel.

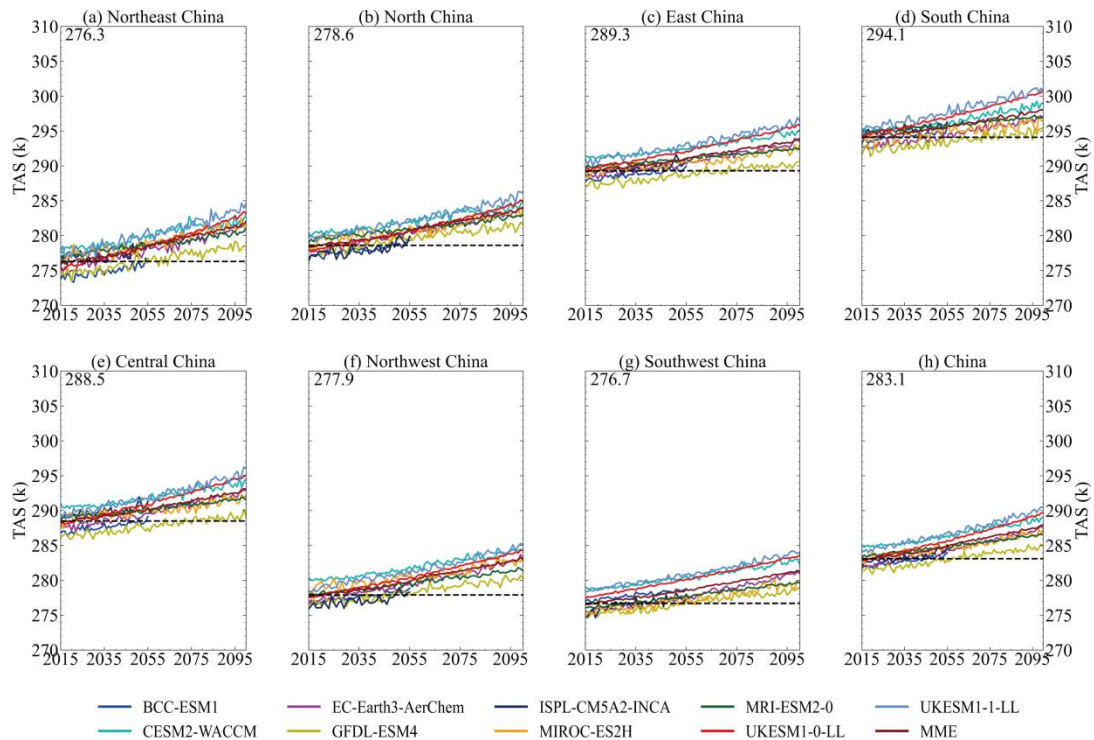


Figure S7 – Changes in the annual mean TAS concentrations for China and sub-regions from 2015–2100, across nine CMIP6 models and MME for the SSP3-7.0 scenario. The black dashed line represents the MME of surface TAS concentrations for 2015–2023, with the value shown in the top left of each panel.

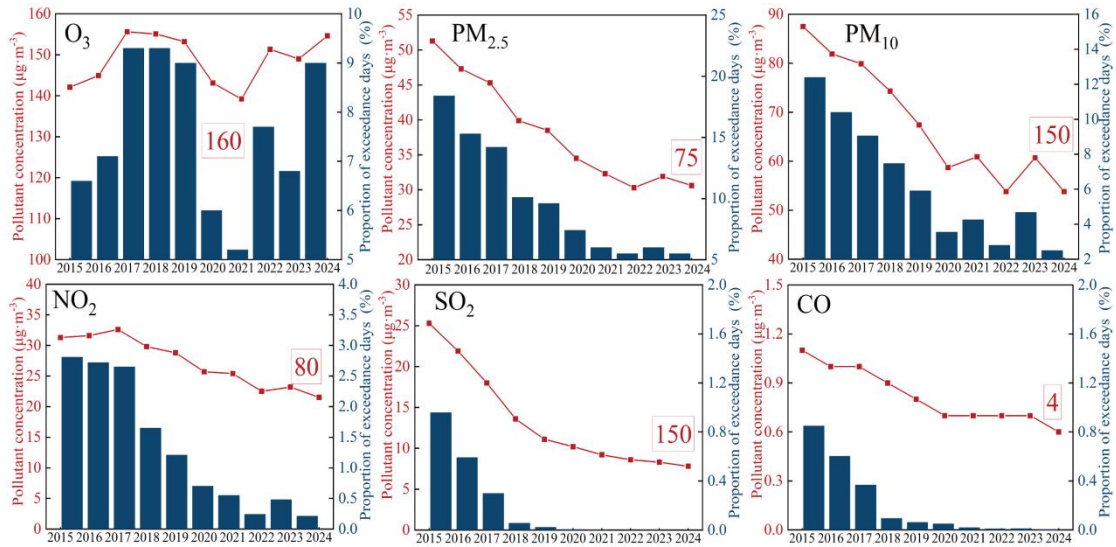


Figure S8 – The average pollutants concentrations (red lines) and the proportion of exceeding the standard (blue bars) in China during 2015–2024, based on ground-based observational data from 1181 monitoring stations of the China National Environmental Monitoring Centre (CNEMC, <http://www.cnemc.cn/sss/j>). O₃ represents the 90th percentile of MDA8 ozone concentrations, and CO represents the 95th percentile of daily mean CO concentrations. Values within the boxes indicate the concentration limits according to the Chinese Ambient Air Quality Standards.

Table S1 – CMIP6 variables and auxiliary datasets used in this study.

Variable name	Source	Temporal resolution	Purpose in the analysis	Reference
Ozone	CMIP6 models	Amon	O ₃ analysis	Eyring et al. (2016)
	TAP dataset	Mon	Uncertainties analysis	Xue et al. (2020)
	Ground-based observations	Mon (derived from hourly)	O ₃ -NO ₂ -NMVOCs relationship	Li et al. (2017)
NO _x	CMIP6 models	Amon	Correlation analysis	Collins et al. (2017)
	Ground-based observations	Mon (derived from hourly)	O ₃ -NO ₂ -NMVOCs relationship	Li et al. (2017)
TAS	CMIP6 models	Amon	Correlation analysis	Eyring et al. (2016)
CH ₄	CMIP6 models	Amon	Correlation analysis	Collins et al. (2017)
NMVOCs (emivoc)	CMIP6 models	Amon	Correlation analysis	Collins et al. (2017)
BVOCs (emibvoc)	CMIP6 models	Amon	Correlation analysis	Collins et al. (2017)
Surface types	MODIS/MCD12Q1	2020 (fixed)	Uncertainties analysis	Friedl and Sulla-Menashe (2019)
Total cloud cover	ERA5 (ECMWF)	Mon	Uncertainties analysis	Wu et al. (2023)
PM _{2.5} and its components	TAP dataset	Mon	Uncertainties analysis	Xiao et al. (2022)

Table S2 – Summary of seasonal performance statistics of MME O₃ relative to TAP.

Statistics ($\mu\text{g}\cdot\text{m}^{-3}$)	MAM	JJA	SON	DJF
Bias	-25.4	-12.8	-22.9	-25.3
SD (Inter-model)	16.8	18.8	15.2	19.0

Table S3 – Annual correlation coefficients (r) between individual CMIP6 models and TAP.

Models	BCC-ESM1	CESM2-WACCM	EC-Earth3-AerChem	GFDL-ESM4	IPSL-CM5A2-INCA	MIROC-ES2H	MRI-E SM2-0	UKESM 1-0-LL	UKESM 1-1-LL	MME
r	0.78	0.91	0.77	0.80	0.80	0.88	0.81	0.73	0.74	0.80

Table S4 – Meaning and characteristics of typical scenarios in CMIP6 in this study

(Global warming levels are based on the IPCC AR6 assessments of CMIP6 model projections (2081–2100 vs. 1850–1900) with likely (5–95 %) ranges. Scenarios marked * are research variants and not part of the five core SSP scenarios.)

Scenario	Socioeconomic Pathway	2100 Radiative Forcing ($\text{W}\cdot\text{m}^{-2}$)	Global Warming in 2100 ($^{\circ}\text{C}$, relative to 1850–1900)	Emission Trends & Policy Features	Typical Applications / Notes	Reference
SSP1-1.9	Sustainable development (green growth, low inequality, high tech)	≈ 1.9	$\sim 1.5^{\circ}\text{C}$ (likely range: $1.2\text{--}1.7^{\circ}\text{C}$)	Strong mitigation; net-zero before 2050	1.5°C pathway for Paris Agreement evaluation	Riahi et al. (2017)
SSP1-2.6	Sustainable development (same as SSP1)	≈ 2.6	$\sim 1.8^{\circ}\text{C}$ (likely range: $1.37\text{--}2.4^{\circ}\text{C}$)	Clean energy transition; moderate mitigation	Low-emission sustainable development scenario	IPCC AR6 WGI (2021)
SSP2-4.5	Medium pathway (current trends, moderate mitigation)	≈ 4.5	$\sim 2.7^{\circ}\text{C}$ (likely range: $2.1\text{--}3.5^{\circ}\text{C}$)	Limited global cooperation; gradual emission slowdown	Baseline “medium emission” scenario	Riahi et al. (2017)
SSP3-7.0	Regional rivalry (fragmented development, low cooperation)	≈ 7.0	$\sim 3.6^{\circ}\text{C}$ (likely range: $2.8\text{--}4.6^{\circ}\text{C}$)	Developing countries grow rapidly; fossil fuels dominate	Used as pessimistic reference scenario	IPCC AR6 WGI (2021)
SSP3-7.0-1owNTCF*	Same as SSP3-7.0 but with NTCF control	≈ 7.0	Not officially assessed in AR6	Stronger control of CH ₄ , NMVOCs, BC	Research variant; not an IPCC core scenario; temperature response varies by model	Lund et al. (2020)
SSP4-3.4	Inequality pathway (widening North–South gap)	≈ 3.4	$\sim 2.3^{\circ}\text{C}$ (likely range: $1.9\text{--}2.8^{\circ}\text{C}$)	Developed countries reduce emissions; developing nations increase	Medium-low emission; studies of inequality impacts	O’Neill et al. (2017)
SSP4-6.0	Same as SSP4 but with higher global emissions	≈ 6.0	$\sim 3.0^{\circ}\text{C}$ (likely range: $2.8\text{--}4.0^{\circ}\text{C}$)	Strong disparity between high- and low-emission nations	Medium-high emission; reflects global inequality	O’Neill et al. (2017)
SSP5-8.5	Fossil-fueled growth (high growth, no mitigation)	≈ 8.5	$\sim 4.4^{\circ}\text{C}$ (likely range: $3.8\text{--}5.7^{\circ}\text{C}$)	Very high emissions; no climate policies	Extreme high-emission “worst case” scenario	Riahi et al. (2017)
SSP5-3.4-OS*	Fossil-fueled development (tech-optimistic); overshoot pathway	≈ 3.4 (overshoot)	Not officially assessed in AR6	High early emissions; large-scale carbon removal later	Overshoot research scenario; peak warming $>2^{\circ}\text{C}$ then declines; not AR6 official estimate	O’Neill et al. (2016)

Table S5 – Multi-model mean changes in surface ozone concentrations over China and globally under historical and SSP scenarios .

Main Scenario	China (this study; $\mu\text{g}\cdot\text{m}^{-3}$)	Global (Turnock et al., 2020; ppb)
Historical	Increase of 39.3 ± 14.4 since 1850	Increase of 11.7 ± 2.3 since 1850
SSP1-2.6	Decrease of 12.6 ± 3.1 by 2050 Decrease of 25.3 ± 7.2 by 2100	Decrease of 5 ± 1.2 by 2050 Decrease of 9 ± 1.6 by 2100
SSP2-4.5	Decrease of 13.6 ± 7.2 by 2100	Decrease of 4 ± 1.7 by 2100
SSP3-7.0	Increase of 8.4 ± 2.0 by 2050 Increase of 3.9 ± 4.0 by 2100	Increase of 1.6 ± 0.9 by 2050 Increase of 0.6 ± 1.0 by 2100
SSP3-7.0-lowNTCF	Increase of 5.8 ± 1.5 by 2050 Increase of 4.9 ± 2.0 by 2100	Decrease of 2.5 ± 0.5 by 2050
SSP5-8.5	Increase of 6.3 ± 1.6 by 2050 Decrease of 3.4 ± 2.9 by 2100	Increase of 1.4 ± 0.8 by 2050 Decrease of 2.7 ± 1.5 by 2100

Note: Values represent the multi-model mean \pm one SD. Historical changes are reported relative to pre-industrial conditions (since 1850). Future scenario changes are referenced to 2015–2023 for this study and to 2005–2014 for the global estimates from Turnock et al. (2020). Units differ between regional ($\mu\text{g}\cdot\text{m}^{-3}$) and global (ppb) estimates; comparisons are intended to highlight relative magnitude and directional consistency rather than absolute values.

Table S6 – Inter-ensemble variability of surface O_3 under SSP3-7.0 (2015–2023). Quantified as the average monthly SD across ensemble members for each model ($\mu\text{g}\cdot\text{m}^{-3}$).

Models	BCC-ESM1	CESM2-WACCM	EC-Earth3-AerChem	MRI-ESM2-0	UKESM1-0-LL	MME
SD (O_3)	3.3	2.4	2.6	3.9	2.4	2.9

Note: Only models with more than two ensemble members under SSP3-7.0 were included.

References

- Friedl, M. A. and Sulla-Menashe, D.: MCD12Q1 MODIS/Terra+Aqua Land Cover Type Yearly L3 Global 500 m SIN Grid V006 [Data set], NASA Land Processes Distributed Active Archive Center, <https://doi.org/10.5067/MODIS/MCD12Q1.006>, 2019.
- Li, K., Li, J., Wang, W., Tong, S., Liggio, J., and Ge, M.: Evaluating the effectiveness of joint emission control policies on the reduction of ambient VOCs: Implications from observation during the 2014 APEC summit in suburban Beijing, *Atmos. Environ.*, 164, 117–127, <https://doi.org/10.1016/j.atmosenv.2017.05.050>, 2017.
- Lund, M. T., Aamaas, B., Berntsen, T., and Samset, B. H.: A continued role of short-lived climate forcers under the Shared Socioeconomic Pathways, *Earth Syst. Dynam.*, 11(4), 977–993, <https://doi.org/10.5194/esd-11-977-2020>, 2020.

- O' Neill, B. C., Tebaldi, C., van Vuuren, D. P., Eyring, V., Bilir, T. E., Kram, T., Kriegler, E., Lamarque, J.-F., Lowe, J., Meehl, G. A., Moss, R., Riahi, K., and Sanderson, B. M.: The roads ahead: Narratives for shared socioeconomic pathways describing world futures in the 21st century, *Glob. Environ. Change*, 42, 169–180, <https://doi.org/10.1016/j.gloenvcha.2015.01.004>, 2017.
- Riahi, K., van Vuuren, D. P., Kriegler, E., Edmonds, J., O'Neill, B. C., Fujimori, S., Bauer, N., Calvin, K., Dellink, R., Fricko, O., Lutz, W., Popp, A., Crespo Cuaresma, J., KC, S., Leimbach, M., Jiang, L., Kram, T., Rao, S., Emmerling, J., Ebi, K., Hasegawa, T., Havlík, P., Humpenöder, F., De Silva, L. A., Stev, S., Stehfest, E., Bosetti, V., Eom, J., Gernaat, D., Masui, T., Rogelj, J., Strefler, J., Drouet, L., Krey, V., Luderer, G., Harmsen, M., Takahashi, K., Baumstark, L., Doelman, J. C., Kainuma, M., Klimont, Z., Marangoni, G., Lotze-Campen, H., Obersteiner, M., Tabeau, A., & Tavoni, M.: The Shared Socioeconomic Pathways and their energy, land use, and greenhouse gas emissions implications: An overview, *Glob. Environ. Change*, 42, 153–168, <https://doi.org/10.1016/j.gloenvcha.2016.05.009>, 2017.